Robust clay binder for earth-based concrete

Journal Article

Author(s):
Ardant, Daria; Brumaud, Coralie; Perrot, Arnaud; Habert, Guillaume

Publication date:
2023-10

Permanent link:
https://doi.org/10.3929/ethz-b-000618881

Originally published in:
Cement and Concrete Research 172, https://doi.org/10.1016/j.cemconres.2023.107207

Cement and Concrete Research 172 (2023) 107207

Contents lists available at ScienceDirect

Cement and Concrete Research

journal homepage: www.elsevier.com/locate/cemconres

Robust clay binder for earth-based concrete

Daria Ardant [a], Coralie Brumaud [a,*], Arnaud Perrot [b], Guillaume Habert [a]

[a] Institute of Construction and Infrastructure Management, Chair of Sustainable Construction, Swiss Federal Institute of Technology (ETH Zurich), Stefano-Franscini-Platz 5, Zürich 8093, Switzerland

[b] Université de Bretagne Sud, FRE CNRS 3744, IRDL, Lorient, France

ARTICLE INFO

Keywords:
Rheology
Soil suitability
Earth concrete
Yield stress
Compressive strength

ABSTRACT

The use of excavated earth is a circular and carbon neutral solution gaining growing interest. However, its high variability in properties makes it difficult to master as raw materials for construction. The objective of this paper is to highlight the key parameters allowing overcoming the influence of the variability of soil composition on the earth-based concrete properties. We show that the solid volume fraction of clay paste is the key parameter allowing predicting the fresh state properties of the clay binder, whatever the constitutive clay type, whereas the clay activity and the dry density of the material control the compressive strength of the material. These promising results, validated on sludge, pave the way to optimized mix design strategies for robust earth concrete products.

1. Introduction

Due to the expansion of cities, a high volume of excavated earth is produced every year (estimated to tenth of million per year in the specific case of Switzerland) [1–4]. The material flow in cities shows that this resource quantity is huge and appears as the main urban resource [5,6]. This excavated earth as raw material for construction can be seen as the best example of a closed material flow loop with the best recycling potential [2,7]. It can provide one of the building materials with the lowest environmental impact [8,9]. However, to transform this strong potential resource into construction material and upscale production of earth components in cities, the high variability of soil needs to be faced.

Indeed, earth is a non-standard material, with composition linked to its geological history [10–12]. Consequently, the physical and mineralogical properties of earth excavated from different sites differ from one to another [13], and this variability leads to the production of earth-based materials displaying inconstant properties and performances. This lack of robustness is even highly visible at the local scale, where productions have to deal with it to provide robust material for construction [14–17]. Consequently, the production rate is still low [18] leading to less competitive materials than the conventional and standardized ones. Limiting the impact of the soil variability on the final properties of earth-based concrete can help to promote the use of excavated earth as raw materials and increase the production rate.

In the geotechnical field, two main parameters related to the variability seem to affect the final properties of the materials. The most dominant one is the particle size distribution, as it impacts the packing of the soil [10]. The second one is the mineralogical characteristics of the fine particle fraction. Whereas the particle fraction above 100 μm (order of magnitude), which behaviour is mainly governed by gravitational and frictional interactions, shows roughly the same physical and chemical properties whatever the considered soil, the behaviour of particles below 100 μm (i.e. clay and silt fraction) can vary. Indeed, the nature of this fraction can influence the final properties of the earth sample, as the nature of the particles, their chemical structures, and their physical properties impact the colloidal interactions [17,19–22]. The clay properties themselves highly change from one clay to another. For example, kaolinites are composed of one tetrahedral SiO_4 sheet and one octahedral AlO_6 sheet (TO sequence). They have low cation exchange capacity (CEC) and a layer charge close to zero [23]. Thanks to this structure, they have a low affinity to water and keep an interlayer distance of around 7 Å. Illites are non-swelling triple-layer aluminosilicates. Their structures consist of one octahedral AlO_6 sheet surrounded by two tetrahedral SiO_4 sheets (TOT sequence) with an interlayer distance of 10 Å. This interlayer space, too narrow for a water molecule to go in, is occupied by hydrated K+ cations that serve as binding agents between layers preventing any swelling behaviour. They have a moderate CEC, slightly higher than kaolinites, and a strong negative layer charge [24]. Montmorillonites, as illites, are comprised of triple-layer aluminosilicates but with swelling activity. Their external layers are

* Corresponding author.
E-mail address: brumaud@ibi.baug.ethz.ch (C. Brumaud).

https://doi.org/10.1016/j.cemconres.2023.107207
Received 20 May 2022; Received in revised form 3 May 2023; Accepted 18 May 2023
Available online 14 June 2023

stable with low surface activity. However, the internal faces of their layers are way less stable due to an important substitution of cations completed by Ca^{2+}, $Mg^{2+,}$ or Na^{+} cations. These cations have a high hydration capacity, and consequently, water can go easily in the platelets, producing an increase of the interlayer distance after hydration to 14 Å. They have a high CEC, a high specific area, and a low to moderate negative layer charge [24].

Even if earth is one of the oldest materials used by humanity for building purposes, the variability in its properties and the diversity of existing codes and standards [25] makes it difficult to master as raw materials for construction. Therefore, further research is needed to explore its full potential for construction. Looking at ongoing studies on this material, a gap seems to exist between research at material scale and application. On one hand, clay physicochemical properties and mineralogy structures have been highly studied [12,26–31], but these parameters' impact on earth's final properties have not been fully identified. On the other hand, several studies have been done on earth from different sites to define their fresh and hardened properties for building application, but as results are performed at a concrete scale, no relationships can be found between composition and results [32–37].

To reduce the variables, it can be suggested to work on a reduced fraction of the raw earth. As the fine fraction seems to be the key parameter influencing the performances of earth materials [20,38,39], this work will focus on this fraction. This approach can be strengthened because earth concrete and concrete share many similarities [40,41]. Following this statement, it can also be assumed that advances done on cementitious materials might be usable in the earth construction field, moreover for poured earth applications [41–49]. For instance, the solid volume fraction (ϕ) might be an important parameter explaining some fresh and hardened state properties, as for concrete [50–55]. To explore this assumption, this study will focus on nine different rich clay powders varying by their mineralogy and physicochemical properties to highlight the key parameters that could explain fresh and hardened state properties. Common geotechnical properties such as Atterberg limits and methylene blue values were determined and used to develop general observations. Finally, different sludge, waste coming from different quarries, were used to validate the results previously obtained on rich-clay paste.

2. Materials

2.1. Clays

Nine mineral-rich clay powders, sourced from different sites and suppliers and belonging to three main groups of clay (kaolinite, illite, and smectite family), were used in this study (Table 1). This choice allows increasing the investigated parameters such as mineral composition, particle size distribution (PSD), and clay activity, which might affect further results. A mineral and chemical composition analysis were performed on all studied clays. The particle size distribution was measured using an automatic sedimentometer (PARIO Meter, Germany) following the norm ISO 11277:2020 [56]. Clay particles were dispersed using 100 ml of a sodium hexametaphosphate (NaHMP) solution prepared at 5 wt% to limit a potential overestimation of the particle size distribution due to the formation of clay flocs. Measurement was carried out during 8 h, and sieving over 63 μm was performed to determine the fine content. The specific gravity of solid soil was performed with a water pycnometer following the standard ISO 17892-3:2015 [57]. 10 g of clay were placed in the pycnometer and the total weight was recorded. After filling the pycnometer with water, the set-up was put under vacuum until weight stabilization and complete with water to its full volume to be finally weighed again. For the estimation of the activity of clays, the Methylene Blue test was performed according to the standard AFNOR-NF P94-068 [58]. The methylene blue value (MBV) is obtained by reaching the clay saturation point of methylene blue for 5 min. In literature, it has been exposed that the MBV can be linked to the specific surface area of the fine fraction of a soil through a comparison with N_2 adsorption, which is a technique commonly used to measure this value [59–62]. The only difference results into the fact that N_2 method does not take into account internal surface area of soils as N_2 cannot penetrate into inner layers, leading to a better estimation of the swelling clays' SSA with MB measurement [61] . It has also been showed that MB adsorption can give information on cation exchange capacity (CEC) of soil, as dye adsorption onto clay surfaces occurs through the cation exchange in the alumina silicate lattice and the van der Waals forces with the surface SiOH and AlOH of the alumina-lattice [61,63–65]. This measurement can be thus seen as a quick way to get an overview of the cohesion of the fines fraction of soil (below 400 μm according to the literature).

All geotechnical information is gathered in Table 1. Using the Rietveld Methods, the X-ray diffraction powder technique (XRD) showed the main mineralogical components for each studied rich-clay powder. The complete mineralogical composition is given in Table 2.

2.2. Sand

Pure quartz sand, with a granulometric curve from 0.06 to 0.3 mm sourced from Carlo Bernasconi SA (Switzerland), was used to prepare micromortar samples according to ISO 679:2009 [66]. The use of this inert sand with no ion exchange capacity allowed us to eliminate potential other reactions.

2.3. Sludge

Nine sludge from different companies and locations in France and Switzerland were collected. With unknown mineralogical composition, they were used to serve as validation material for the transferability of the methodology to a broader range of materials. According to the sorting, they are composed of particles with a particle size lower than 80 μm (silt fraction). Methylene blue value, Atterberg limits with fall cone dial penetrometer, and specific density with water pycnometer were determined. The obtained results are gathered in Table 3.

3. Experimental procedures

3.1. Normal consistency and liquid limit

In cement field, the consistency of cement is defined as the minimum amount of water required to form a workable paste of standard (or

Table 1
Information and geotechnical parameters of clays studied.

Clay	*Kaolinite KA*	*Kaolinite KF*	*Kaolinite KM*	*Mtm MR*	*Mtm MG*	*Mtm ML*	*Illite IO*	*Illite IR*	*Illite IG*
Supplier	Argile du Bassin Méditerranéen	Dorfner	Manske	Argile du Bassin Méditerranéen	Argile du Bassin Méditerranéen	Argile du Bassin Méditerranéen	Manske	Manske	Manske
Origin	France	China	France	Italy	Italy	Italy	France	France	France
D10	1.78	1.78	1.74	0.31	0.25	0.3	1.81	1.78	0.82
MBV	2.33	1.33	1.66	22	32	21	3.66	3.33	11.66
Relative density	2.59	2.62	2.54	2.46	2.42	2.36	2.71	2.72	2.43

Table 2
Mineralogy composition of the clays studied by X-Ray diffraction.

	KA	*KF*	*KM*	*MR*	*MG*	*ML*	*IO*	*IR*	*IG*
Kaolinite	87.1	87.2	75.4				12.9	14	
Ca-Montmorillonite				65	83.6	67.6			
Illite							66.4	65	29
Muscovite	10.7	3.6	1.6	20	10.7				11.5
Illite-smectite									29.7
Quartz	2.2	4	23	8.3	0	2	15.6	15.6	25.4
Andesine						20.3	1.3	1.3	
Orthoclase					3.77				1.2
Calcite				3.5	1	3.4	3.8	3.6	3.2
Other	0	5.2	0	3.2	1	6.8		0.5	
Total clay fraction	97.8	90.8	77	85	94.3	67.6	79.3	79	70.2

Table 3
Geotechnical parameters of sludge studied here.

Sludge	*K*	*F*	*RF*	*A*	*C*	*S*	*Re*	*S*	*Ka*
Liquid limit	41.39	32.5	51.9	38.28	45.98	40.80	36.5	46.2	32
MBV	0.5	1.66	7	1	3.33	1.33	0.7	1.83	0.19
Relative density	2.666	2.630	2.613	2.612	2.619	2.644	–	–	2.65

normal) consistency. The identification of the water demand of powders is determined according to the Vicat method as described in [50]. The procedure was as following: an increasing amount of water was added to 250 g of powder (clay) mixed with a four-bladed mixing tool connected to a mechanical stirrer (Heidolph, Switzerland) for 3 min at 350 rpm. After mixing, the Vicat truncated cone (Vicatronic, Matest, Switzerland) was filled with the material and placed under the consistency needle (10 mm diameter), and the penetration depth of the needle in free fall was measured. Two measurements have been performed for each clay mix. When a penetration depth of 6 mm was reached, the water content was recorded, and the corresponding solid volume fraction ϕ_c was calculated as follows:

$$\phi_c = \frac{1}{1 + \rho_s W} \tag{1}$$

With ρ_s the absolute density of the powder and W the water content of the mix. At this state, it is admitted that all particles are hydrated and start to be suspended in the aqueous phase [53].

In geotechnical field, the Atterberg limits correspond to the characteristic water content when the soil changes in consistency, from liquid to plastic for the liquid limit (LL) and from plastic to brittle solid for the plastic limit. The liquid limit has been defined with a cone dial penetrometer following the standard ISO 17892-12:2018 [67]. It has been shown that this tool show better accuracy than the Casagrande cup for the determination of the liquid limit, as it does not depend on the operator interpretation [68]. In this paper, a cone dial penetrometer from Matest (Switzerland) equipped with a stainless steel penetration test cone of dimension 35 mm long, 30° angle, for a total tool weight of 80 g was used. The clay powder was manually mixed with water until reaching a homogeneous state, and tested. According to the standard [69], the liquid limit is reached at a 20 mm penetration. After each measurement, a sample of each mix was collected and put in the oven at 105° for the determination of the paste water content. This tool can also define the plastic limit by a log/log extrapolation to reach the value at a 2 mm penetration [70]. The water content to reach the liquid limit was then used to determine the corresponding solid volume fraction to define at which value this state-change might occur. In this paper, the solid volume fraction linked to the liquid limit and calculated with Eq. (1) will be named ϕ_{LL}. Eq. (1) was used to determine the theoretical solid volume fraction (ϕ) of pastes and micromortar: with a maximal particle size below 400 μm, the latter is still in the range of applicability of the cone dial penetrometer measurements [21].

3.2. Yield stress measurements

3.2.1. Fall cone dial penetrometer

The cone dial penetrometer has been exposed as an accurate tool to determine clay paste yield stress if the three following parameters are respected. Firstly, the paste consistency has to be liquid or plastic, as at this stage, it is considered that the friction stress is equal to the shear yield stress of the material [71]. Secondly, the paste tested has to be considered homogeneous at the tested scale. Finally, its largest grain size has not to be higher than 10 % of the height of the cone [21], which in our case represent 400 μm. The equation used to calculate the yield stress at each measured depth has been described in [21].

3.2.2. Rheometer

The rheology measurements were performed using a Malvern Kinexus Lab + (Malvern Instruments, Switzerland) stress-controlled rheometer equipped with vane geometry [72]. The vane geometry consisted of a four-bladed paddle with a diameter of 14 mm, the outer cup diameter was 25 mm, and its depth 63 mm. This geometry was chosen to minimize the disturbance of the material during the introduction of the tool and avoid the wall slip effect [73]. The setup was kept at a constant temperature of 23 ± 0.1 °C with a thermostatic bath during the measurement. The measurement procedure was similar to the one used in Perrot et al. [74]. The clay was first mixed with water at different water to clay ratios for 1 min. Directly after mixing, the cup was filled and covered with a trap cover to limit evaporation. After 1 min of resting to avoid disturbance, a shear rate of 0.01 s^{-1} was applied to the sample 240 s. Viscosity effects are negligible at such a low shear rate, and yield stress could be computed from the measured torque peak value at flow onset [54]. For each mix, yield stress measurement was performed three times to improve accuracy.

3.3. Compressive strength and dry density

Compressive strength tests were performed to investigate the influence of clay nature and water content on the mechanical performance of clay and sludge micromortars. To limit the potential shrinkage of clay samples, clay paste was mixed with an inert quartz fine sand to measure the hardened state. For all mixes, the volume ratio between paste and sand was kept constant at 40/60. At least three different water ratio were used. Taking into account the initial composition of sludge, a constant mass ratio of 50/50 was defined, and the three different water content was tested. The clay mortars were prepared using the following

procedure: water was mixed with dry components (clay or sludge and quartz sand previously homogenized) in an automatic mortar mixer (Matest, Switzerland) during 2 min at low speed (62 rpm) with planetary action. After the mixing stage, a standard prismatic formwork of dimensions 40 × 40 × 160 mm^3 was filled with the clay micromortar. Samples were dried for two days at ambient air condition, demolded, and put into the oven at 105 °C until weight stabilization. Compression test measurements were repeated six times for each clay-based mortar sample, and four times on each sludge based mortar sample.

The dry density of the samples was measured following the protocol of hydrostatic weighing based on Archimede's principle. The tested material was sampled from the resting bar used for the compression test. A coating made of a known mass of varnish was applied to the material. The sample was then weighed in air and water, and the density was calculated. This measurement was repeated three times to ensure the accuracy of the results.

4. Results and discussion

4.1. Water demand and solid volume fraction

In the concrete field, the solid volume fraction (ϕ) is an important parameter for the determination of an optimized mix design [52]. At the paste scale, the parameter ϕ_c is kept as a reference point, as it represents the normal consistency when all particles are hydrated and start to be suspended in the aqueous phase [53]. In the geotechnical field, a similar consistency refers to the liquid limit, as this limit corresponds to the state where particles start to be in suspension within the system (defined here as the solid volume fraction ϕ_{LL}). These two solid volume fractions, determined thanks to the normal consistency (ϕ_c) test and to the penetrometer (ϕ_{LL}) for all the clays, are plotted in Fig. 1 for comparison.

A good correlation exist between these two parameters, whatever the considered clay group. If we focus now on a specific clay type group, it can be observed that montmorillonites, due to their swelling capacity, have the lowest characteristic solid volume fraction, kaolinites have relatively close solid volume fractions, and illites do not follow a common trend. The orange and red ones (IR and IO) have the highest solid volume fraction and close results. This can be explained by the potassium bonding between the clay layer structure, limiting the possibility for water to penetrate the clay platelet [19]. However, the green illite shows results between illites and montmorillonites, close to kaolinites, which is coherent knowing its mineralogy (i.e. interstratified illite-smectite clay). This observation confirms that the mix design strategy currently applied for cementitious materials can be transferred to clay-based materials. The solid volume fractions observed in Fig. 1 seem to be particularly low when considering clay as plate like particles. This can be explained by the random network configuration of the clay platelets and the swelling capacity of some of them. Indeed, it is known that the clay platelet charges can evolve with external condition such as the pH of the interstitial solution [12,31,75,76]. By mixing clay with tap water, clays platelets are mostly arranged in an house of cards structure, leading to a high microporosity and consequently to a low solid volume fraction. Modifying the pH of the solution leads to a clay particles reorganization with a potential improvement of the packing. This optimization can also be done through the addition of mineral dispersant [43,46,48].

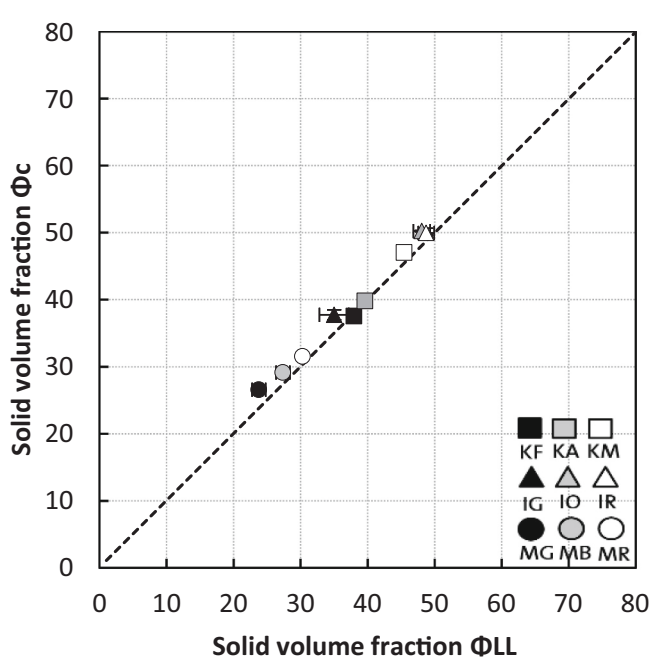

Fig. 1. Relationship between the solid volume fraction ϕ_c measured through the paste consistency protocol and the solid volume fraction ϕ_{LL} calculated from the water moisture corresponding to the liquid limit state.

4.2. Yield stress of clay pastes

Perrot et al. [21] showed that the fall cone dial penetrometer can be used for the determination of the yield stress of clay pastes when the considered paste is in its liquid or plastic state. For instance, with the equipment used, a clay paste at its liquid limit reaches a yield stress of 2275 Pa. However, this tool cannot be used for paste with yield stress lower than 750 Pa as the paste consistency becomes too soft to have enough friction to hold the needle before the end of the cup. Therefore, to obtain the yield stress value at the lowest solid volume fraction, measurements were performed on rheometer through a flow onset protocol. Indeed, results from rheometer and fall cone for yield stress values are in good agreement [21]. The yield stress of clay pastes, calculated from the fall cone dial penetrometer measurements [21] (Fig. 2a) measured with the rheometer is plotted as a function of the corresponding solid volume fraction.

In literature, the yield stress of particles in suspension has been modelled. The model showing the best accuracy for a high range of solid volume fraction is the yield stress model (YODEL) proposed by Flatt and Bowen [54]. Although the YODEL model was first developed to predict the yield stress of spherical-like particles in suspension such as cement grain or alumina powder, it has already been applied with good accuracy on kaolinite platelet [44]. For such a system, the equation used is written as follows:

$$\tau_0 = m_1 \frac{\phi^2(\phi - \phi_p)}{\phi_m(\phi_m - \phi)} \tag{2}$$

where ϕ_m is the dense packing fraction, ϕ_p is the percolation threshold corresponding to the solid volume fraction when a yield stress starts to be observed (i.e. solid volume fraction at which the particles start to interact), ϕ is the solid volume fraction corresponding to the calculated yield stress and m_1 a factor that describes the global interactions between clay particles. This factor simplifies a part of the basic expression of the YODEL, as all interactions become more difficult to model on heterogeneously charged platelets [44]. For high solid volume fraction, the equation is simplified, as the influence of the percolation threshold becomes negligible [54].

$$\tau_0 = m_1 \frac{\phi^3}{\phi_m(\phi_m - \phi)} \tag{3}$$

This model is fitted to the experimental data obtained with the penetrometer (Fig. 2a) and with the rheometer (Fig. 2b). However, ϕ_m is not a well-defined parameter in earth construction. Based on Perrot et al. [44], it can be suggested that the ϕ_m value for clay might be lower than the ϕ_m for spherical particles because of the clay particle aspect ratio,

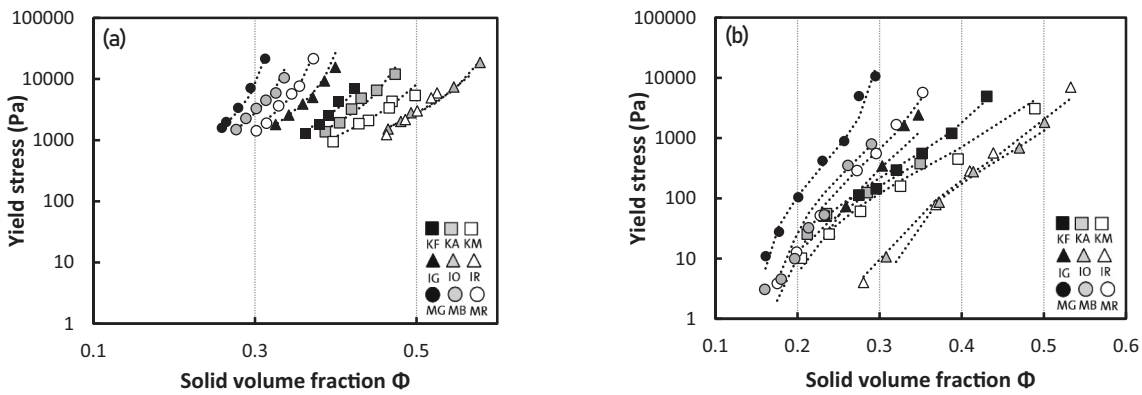

Fig. 2. Yield stress evolution of clay pastes measured with (a) fall cone and (b) rheometer as a function of their solid volume fraction. The dotted lines are the predictions of the YODEL.

and that ϕ_m might be equivalent to ϕ_{PL} [44]. It has also been exposed that when ϕ_{LL} is used to normalized the solid volume fraction of paste with consistency measurable on penetrometer, the yield stress evolution overlapped for all ϕ/ϕ_{LL} values [77]. Based on this statement, we can expect a ϕ_m value written in relationship with ϕ_{LL}.

By applying the relationship $\phi_m = \phi_{LL}/0.86$, the value of ϕ_m obtained seems to follow the ϕ_m values found in literature for kaolinite particles [44]. The maximum solid volume fractions obtained for montmorillonites and illite IG are lower than those obtained for illites IR, IO, and kaolinites. This high variation of ϕ_m between illites, kaolinites and montmorillonites can be the consequence of the clay swelling capacity.

By fixing the dense solid volume fraction ϕ_m, it is then possible to adjust other parameters. The only parameter fitted for high solid volume fractions is the factor m_1, combining the existing interaction forces between clay particles. For low solid volume fractions, the percolation threshold is then the parameter that has the major impact. The simplified version of the YODEL model (Eq. (3)) has been plotted for each clay paste (cf. Fig. 2).

To get rid of the influence of the high change in ϕ_m, and have a better view of the yield stress evolution, the solid volume fraction of each mix has been normalized. In Fig. 3 (b), for mixes with a solid volume fraction higher than 0.75 ϕ/ϕ_m, all clays show the same behaviour in terms of yield stress evolution. This result follows the YODEL as the m_1 factor seems to be constant whatever the considered type of clay. Finding that the global interaction between particles will be the same for each clay powder studied here was not expected, knowing the variability of their composition. These interactions are more difficult to model for clay platelets than for spherical ones. A complete description of these interactions is out of the scope of this article and will need further research to be confirmed. However, it can be exposed here that these parameters do not seem to create a divergence between clay paste at these solid volume fractions and can be simplified by a single value $m_1 = 1.5$.

For mixes with a solid volume fraction lower than 0.75 ϕ/ϕ_m, divergence can be seen between kaolinites and other clays. It is worth noting that this range of volume fraction providing low yield stress values is of interest when mix-designing self-compacting or poured earth. Kaolinites need a higher reduction of solid volume fraction to reach an equivalent yield stress. At this solid volume fraction range, the percolation threshold is a predominant parameter influencing the YODEL. By looking at the relationship between ϕ_m and ϕ_p, two trends can be seen and might explain this difference. Illites and montmorillonites show a ϕ_p much closer to their ϕ_m than kaolinites. Indeed, the kaolinite platelets can easily go to a house of card structure when the paste is at a pH at 7 [12,44,46], which is the case here. This attraction between edges and faces leads to the creation of flocs that entrapped water and can form a resistant microstructure at lower solid volume fraction. The initial version of YODEL provided by Eq. (1) is compared with measured yield stress values using the rheometers for a percolation threshold of $0.3\phi_m$ for kaolinites and of $0.48\phi_m$ for illites and montmorillonites in Fig. 4.

Here again, it is remarkable that the YODEL model is able to predict the yield stress of all tested clays with the same pre-factor m_1 value and microstructure descriptions parameters only related to the liquid limit values. These experimental observations pave the way to a simplified and generalized use of the YODEL model in the case of clay binders. It can be suggested that working with a paste with high solid volume fraction can help to overcome the impact of the variability on yield stress definition.

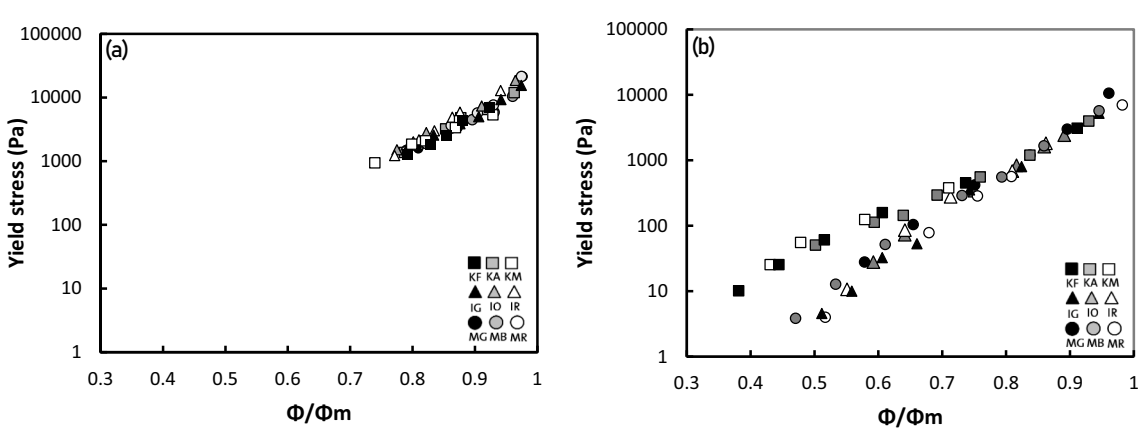

Fig. 3. Yield stress evolution of clay pastes measured with (a) fall cone and (b) rheometer as a function of ϕ/ϕ_m.

4.3. Hardened state properties.

In Fig. 5, the compressive strength of the different clay mortar samples is plotted as a function of their respective dry density. For a given clay group, a correlation between the compressive strength and the dry density exists. The mechanical resistance decreases with a decreasing in density. This general observation is well-known in the earth construction field [35,36,78]. However by comparing the different clay binder, no general trends can be seen, leading to the possibility that other parameter might act on the compressive strength value.

This other parameter can be the binder activity. The literature has exposed that soils with high activity are more cohesive than soils with low activity [10,20,24,38]. Looking at the results in Figs. 4 and 5, this parameter could explain why kaolinites show a lower compressive strength than montmorillonites, even if they have a higher dry density. Following this hypothesis, the MBV of all micromortar samples has been measured and used to divide the compressive strength (Fig. 6). As expected, the binder activity has an impact on clay micromortar compressive strength. All micromortars show a general trending curve, even if clays can easily be sorted by type. As montmorillonites have a high MBV, when this value is used to divide their compressive strength, the obtained results are low and seem more likely to follow their low dry density. In opposition, kaolinites have a low MBV value and a low compressive strength. The illites relationship between MBV and compressive strength still gives high results, as their compressive strength is high enough to not drop with their MBV value.

The dry density of the sample and the particle density can be used to determine the porosity (n) and the theoretical solid volume fraction ($n = 1 - \rho_d/\rho_s$, where ρ_d the dry density of the sample and ρ_s the absolute density of the powder). Knowing that the porosity is related to the solid volume fraction ($\phi = 1 - n$), it can be expected that a same general relationship between solid volume fraction, compressive strength, and MBV exists, as the one exhibited with the dry density. To confirm this hypothesis, the theoretical solid volume fraction of each mix (assuming a water saturated material) has been calculated thanks to the water to solid ratio, as shown in Section 3.2 (Fig. 6b). Results showed a good accuracy until a certain value of solid volume fraction. This difference can be explained by how the theoretical solid volume fraction is determined. By working with dense suspension, it is supposed that water fills all the pores leading to the known relationship between solid volume fraction, water content, and particle density [53]. However, when the solid volume fraction becomes too high, the pores between particles might not be fully saturated, leading to an underestimated porosity and, consequently, an overestimated solid volume fraction. This assumption is confirmed as the mixes showing a drop in compressive strength have a theoretical solid volume fraction higher than their dense solid volume fraction. Knowing that this limit can be exposed at the maximum packing where all particles are hydrated, and thus where Eq. (1) is valid, having a mix with higher solid content might significate that all pores are not filled with water, leading to this overestimation of the solid volume fraction disconnected to the porosity. In the end, it can be suggested that, by knowing the water to solid ratio, the particle density, which are the data needed to calculate the theoretical solid volume fraction, and the MBV of a clay micromortar, it becomes possible to anticipate its compressive strength after drying at 105 °C. This relationship seems to be true as long as the solid volume fraction of the paste is below ϕ_m.

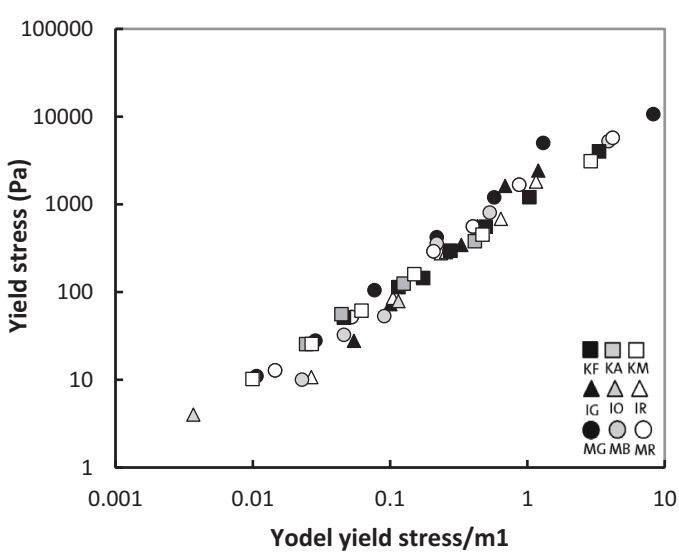

Fig. 4. Dimensionless yield stress prediction compared to yield stress measurements. m_1=1.5 Pa; $\phi_m = 0.86\phi_{LL}$; $\phi_p = 0.3\phi_m$ for kaolinites and $\phi_p = 0.48\phi_m$ for illites and montmorillonites.

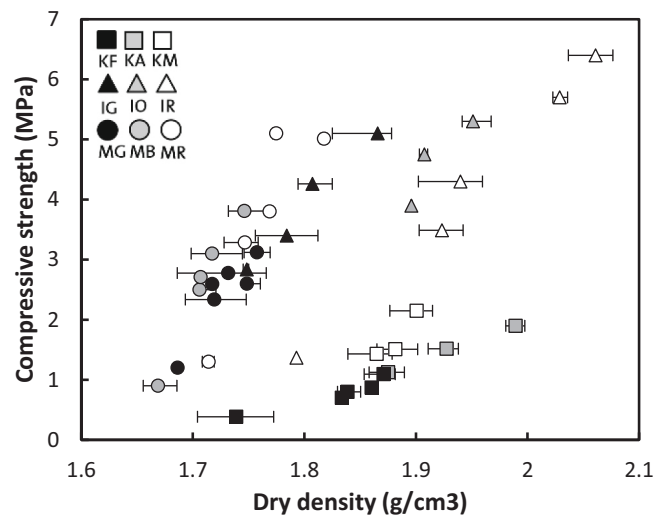

Fig. 5. Compressive strength as a function of the dry density for all studied mixes.

A parallel can be drawn with concrete technology for which the compressive strength can be predicted from the binder activity (class of cement) and a term linked to the porosity of the cement paste (commonly linked to the water to cement ratio). The results shown here demonstrate that the compressive strength of the earth mortar is the product of the clay activity (MBV) by a function of the porosity, which is directly related to the dry density of the material.

It is worth noting that, as the MBV is related to the specific surface area of soil particles, it can thus reflect the particle size distribution and the particle shape, which directly influence the pore structure. Indeed, according to Van Damme et al. [79], the origin of the strength (so-called cohesion in their work) of earth-based materials is due to capillary forces that are strongly linked to pore geometries. This statement could explain why the MBV seems to be strongly linked to the compressive strength of earthen materials.

4.4. Application

The fresh and hardened state properties of clay binders seem to be highly related to their solid volume fraction. The general trends found can help to tackle the variability of clay to provide a robust binder. However, this work has still been performed on a known binder and defined micromortar. To confirm these results, the yield stress and the compressive strength of several unknown sludge have been compared in the same way as the rich clay ones (Fig. 7). The yield stress has been calculated thanks to the fall cone test on sludge paste with three different water content. A relationship between particles size and yield

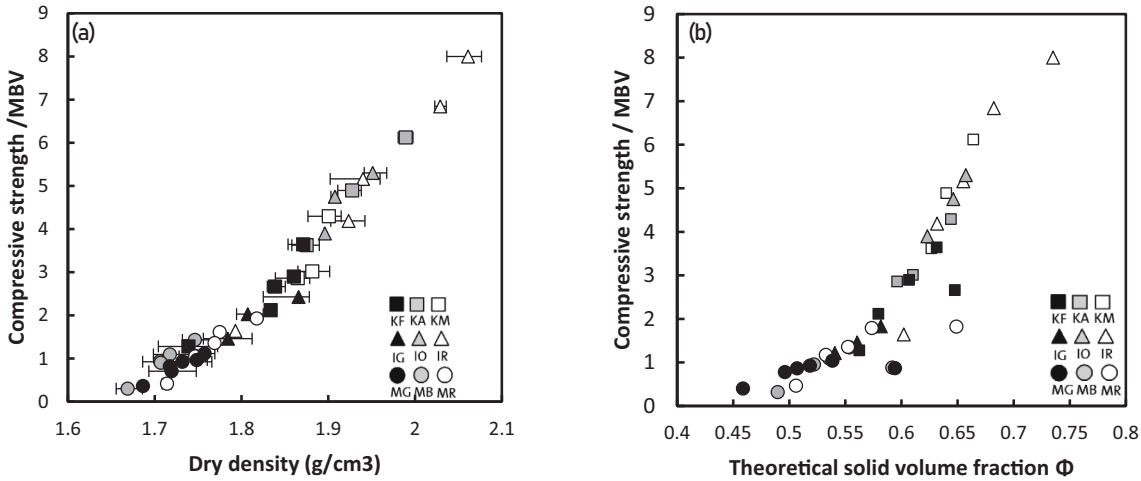

Fig. 6. Clay micromortar compressive strength divided by the corresponding MBV (a) as a function of the dry density and (b) as a function of the theoretical solid volume fraction.

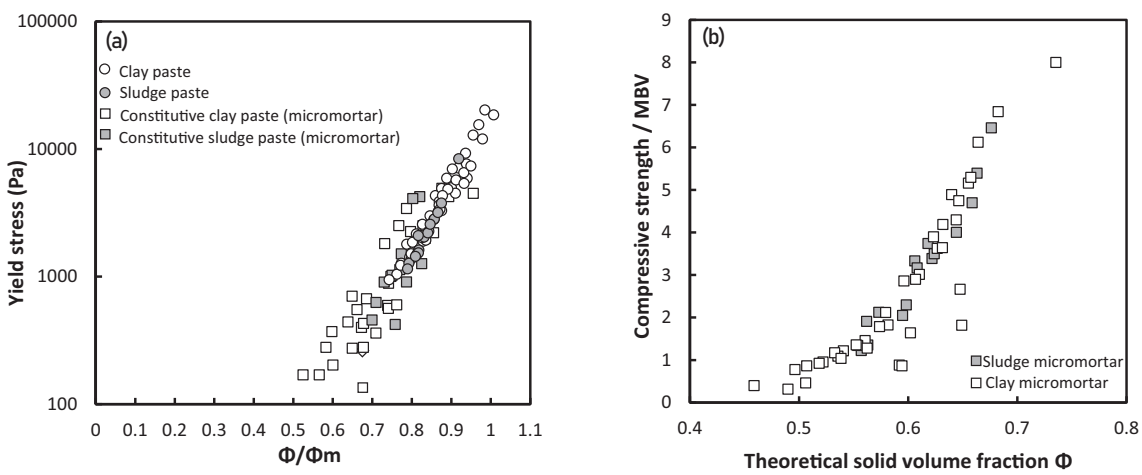

Fig. 7. (a) Yield stress of pastes and constitutive pastes of micromortar as a function of ϕ/ϕ_m and (b) compressive strength normalized by the MBV as a function of the theoretical solid volume fraction of sludge and clay paste.

stress has already been exposed in literature [80] and models developed for yield stress suspending fluids can be used to predict the effect of these inert particles [81]. This model has been used to confirm the correlation between yield stress of the paste and the yield stress of the paste of the micromortar computed from micromortar yield stress thanks to the Mahaut et al. model [69] (Fig. 7a). Results show that these models seem to be applicable with a good accuracy to rich clay binder and mortar. The small dispersion observed between experimental values can be the consequence of the particle size of the sand fraction. With a small particle size for inert particles, the model becomes less accurate as smaller particles can be in the range of the particle size of the paste.

In further work, it could be interesting to work at the different scales of particles size as commonly done in concrete science [82–84]. However, by comparing results from sludge and clay paste, no difference can be seen in the yield stress evolution when solid volume fraction is normalized by ϕ_m.

To look at the hardened state correlation exposed in Section 4.2, the MBV has been taken into account (Fig. 7b). It is observed that micromortar, unknown sludge and known clay micromortars present a similar behaviour. It can be noted that all sludge fall on the theoretical trend line, suggesting that they are water saturated. Additionally, it is worth to mention (not plotted here) that, as in Fig. 6. (a), all points of the compressive strength/MBV versus dry density graph fall on the same curve.

It can thus be suggested that a sorting <300 μm allows highlighting the key parameters that could master the variability of the fine fraction. Finer sieving might not be mandatory. This application on sludge confirms that key parameters allowing mastering the variability of the earth are the binder's activity, determined through the MBV, and the dry density of the material. Other binder characteristics do not seem to influence these properties. It also confirms that models used for cement paste and concrete seems to be applicable on earth paste and mortar.

5. Conclusion

Thanks to its low environmental impact and its high availability, earth is a promising building material. However, as its composition is linked to its geological history, the mineralogical and geotechnical properties of earth highly varies. This variability creates a high deviation in fresh and hardened properties of the final earth concrete products. To reduce the amount of parameters, this work focused only on the fine fraction of the earth, the clay, and highlighted some key parameters allowing the prediction of earth binder properties, at fresh and hardened state.

At fresh state, for a solid volume fraction higher than 0.75 ϕ/ϕ_m, YODEL model is able to predict the yield stress of all tested clays with the

same pre-factor m_1 value and microstructure descriptions parameters only related to the liquid limit values, whatever the considered clay group. However, below this fraction, the behaviour of the clay materials is dependent on the clay mineralogical nature. The main difference between kaolinites and other clays tested seems to be the consequence of the ϕ_p. Kaolinites shows a ϕ_p much closer to ϕ_m in comparison with other clays. The relationship between paste yield stress and mortar yield stress seems to confirm following model developed for concrete field. At hardened state, two parameters seems to control the behaviour of the material when it is dried at 105 °C. The dry density of the mix, which is directly linked to the material mix-design when the solid volume fraction of the material is below ϕ_m; and the clay activity, which can be determined thanks to the methylene blue value. By getting these two parameters, it becomes possible to anticipate the compressive strength of a clay micromortar. More information on the fine fraction does not seem important to get for these properties as same trends can be seen on sludge with unknown properties. However, even if the variability of earth binder starts to be tackled to provide a robust mix design, the impact of other fractions composing earth-based concrete still need to be better understood to use excavated earth as raw material for robust construction material.

CRediT authorship contribution statement

Daria Ardant: Conceptualization, Methodology, Investigation, original draft preparation, Writing and- Reviewing.

Coralie Brumaud: Conceptualization, Methodology, Supervision, original draft preparation, Writing- Reviewing and Editing.

Arnaud Perrot: Conceptualization, Methodology, Reviewing.

Guillaume Habert: Conceptualization, Methodology, Supervision, Reviewing.

Declaration of competing interest

The authors declare that they have no known competing financial interests or personal relationships that could have appeared to influence the work reported in this paper.

Data availability

No data was used for the research described in the article.

References

[1] K. De Cooman, Down to earth: BC materials transforms urban excavated earth into building materials, in: LEHM 2020 – 8th Int. Conf. Build. with Earth, OnlineDachverband Lehm e.V., Weimar, 2020.

[2] A. Klinge, E. Roswag-Klinge, L. Radéljic, D. Bojic, E. Neumann, Earthen building materials as an opportunity to reduce mineral construction and demolition waste (CDW), in: LEHM 2020 – 8th Int. Conf. Build. with Earth, OnlineDachverband Lehm e.V., Weimar, 2020.

[3] Das KAR-Modell – Kies-, Aushub- und Rückbaumaterialflüsse, (n.d.).

[4] H. Dahlbo, J. Bachér, K. Lähtinen, T. Jouttijärvi, P. Suoheimo, T. Mattila, S. Sironen, T. Myllymaa, K. Saramäki, Construction and demolition waste management - a holistic evaluation of environmental performance, J. Clean. Prod. 107 (2015) 333–341, https://doi.org/10.1016/j.jclepro.2015.02.073.

[5] C. Llatas, A model for quantifying construction waste in projects according to the European waste list, Waste Manag. (2011), https://doi.org/10.1016/j.wasman.2011.01.023.

[6] C.S. Vieira, P.M. Pereira, Use of recycled construction and demolition materials in geotechnical applications: a review, Resour. Conserv. Recycl. (2015), https://doi.org/10.1016/j.resconrec.2015.07.023.

[7] E. Hamard, B. Lemercier, B. Cazacliu, A. Razakamanantsoa, J.C. Morel, A new methodology to identify and quantify material resource at a large scale for earth construction – application to cob in Brittany, Constr. Build. Mater. (2018), https://doi.org/10.1016/j.conbuildmat.2018.03.097.

[8] A. Shukla, G.N. Tiwari, M.S. Sodha, Embodied energy analysis of adobe house, Renew. Energy (2009), https://doi.org/10.1016/j.renene.2008.04.002.

[9] J.C. Morel, A. Mesbah, M. Oggero, P. Walker, Building houses with local materials: means to drastically reduce the environmental impact of construction, Build. Environ. (2001), https://doi.org/10.1016/S0360-1323(00)00054-8.

[10] N.C. Brady, R.R. Weil, The Nature and Properties of Soils, 15th edition, Colombus, 2016.

[11] European Commission, Soil Atlas of Europe, European Soil Bureau Network, 2005.

[12] Romain Anger, Approche granulaire et colloïdale du matériau terre pour la construction, INSA, 2011.

[13] A. Azil, M. Le Guern, K. Touati, N. Sebaibi, M. Boutouil, F. Streiff, S. Goodhew, M. Gomina, Earth construction: field variabilities and laboratory reproducibility, Constr. Build. Mater. (2022), https://doi.org/10.1016/j.conbuildmat.2021.125591.

[14] H. Gasnier, Construire en Terres d'excavation, un Enjeu Pour la Ville Durable, Université Grenoble Alpes (ComUE), 2019.

[15] S. Guihéneuf, Formulation et Renforts de Blocs en Matériau Terre Pour une Utilisation Structurelle, Rennes, INSA, 2020.

[16] K.A.J. Ouedraogo, Stabilisation de Matériaux de Construction Durables et Écologiques à Base de Terre Crue par des Liants Organiques et/ou Minéraux à Faibles Impacts Environnementaux, Université Paul Sabatier, Toulouse III, 2019.

[17] T. Vinceslas, Caractérisation D'éco-Matériaux Terre-Chanvre en Prenant en Compte la Variabilité des Ressources Disponibles Localement, Université Bretagne Sud, 2019.

[18] Guide de Conception et Construction CycleTerre, Guid. Concept. Constr. CycleTerre. https://www.cycle-terre.eu/wp-content/uploads/2021/06/CycleT_Guide-de-conception-et-construction_COMPLET_BD.pdf, 2021.

[19] L. Fontaine, R. Anger, Bâtir en terre / du grain de sable à l'architecture, du grain de sable à l'architecture, in: Laetitia Fontaine, Romain Anger (Eds.), Belin, Beaux Livres Be, 2009 (9782701152042 - Leslibraires.fr).

[20] M. Lagouin, J.E. Aubert, A. Laborel-Préneron, C. Magniont, Influence of chemical, mineralogical and geotechnical characteristics of soil on earthen plaster properties, Constr. Build. Mater. 304 (2021), https://doi.org/10.1016/j.conbuildmat.2021.124339.

[21] A. Perrot, D. Rangeard, T. Lecompte, Field-oriented tests to evaluate the workability of cob and adobe, Mater. Struct. Constr. 51 (2018) 1–10, https://doi.org/10.1617/s11527-018-1181-4.

[22] S. Guihéneuf, D. Rangeard, A. Perrot, Processing methods for optimising the mechanical strength of raw earth-based materials, Proc. Inst. Civ. Eng. - Constr. Mater. (2020) 1–11, https://doi.org/10.1680/jcoma.19.00115.

[23] M. Schmid, J. Plank, Interaction of individual meta clays with polycarboxylate (PCE) superplasticizers in cement investigated via dispersion, zeta potential and sorption measurements, Appl. Clay Sci. 207 (2021), https://doi.org/10.1016/j.clay.2021.106092.

[24] J.M. Huggett, Clay Minerals, Elsevier Inc., 2004, https://doi.org/10.1016/B0-12-369396-9/00273-2.

[25] A. Fabbri, J.C. Morel, J.E. Aubert, Q.B. Bui, D. Gallipoli, B.V.V. Reddy, Testing and Characterisation of Earth-based Building Materials and Elements: State-of-the-Art Report of the RILEM TC 274-TCE, 2022.

[26] B. Velde, Clays as minerals, in: Introd. to Clay Miner., Springer, Netherlands, 1992, pp. 41–100, https://doi.org/10.1007/978-94-011-2368-6_3.

[27] D. Tessier, Behaviour and Microstructure of Clay Minerals, in: M.F. De Boodt, M.H. B. Hayes, A. Herbillon, E.B.A. De Strooper, J.J. Tuck (Eds.), Soil Colloids Their Assoc. Aggregates, Springer US, Boston, MA, 1990, pp. 387–415, https://doi.org/10.1007/978-1-4899-2611-1_14.

[28] M.F. Brigatti, E. Galan, B.K.G. Theng, Chapter 2 structures and mineralogy of clay minerals, Dev. Clay Sci. 1 (2006) 19–86, https://doi.org/10.1016/S1572-4352(05)01002-0.

[29] G. Wang, L. Ran, J. Xu, Y. Wang, L. Ma, R. Zhu, J. Wei, H. He, Y. Xi, J. Zhu, Technical development of characterization methods provides insights into clay mineral-water interactions: a comprehensive review, Appl. Clay Sci. 206 (2021), 106088, https://doi.org/10.1016/j.clay.2021.106088.

[30] J.R. Clausell, C.H. Signes, G.B. Solà, B.S. Lanzarote, Improvement in the rheological and mechanical properties of clay mortar after adding Ceratonia Siliqua L. extracts, Constr. Build. Mater. 237 (2020), https://doi.org/10.1016/j.conbuildmat.2019.117747.

[31] Y. Du, C. Brumaud, F. Winnefeld, Y.H. Lai, G. Habert, Mechanisms for efficient clay dispersing effect with tannins and sodium hydroxide, Colloids Surf. A Physicochem. Eng. Asp. 630 (2021), 127589, https://doi.org/10.1016/J.COLSURFA.2021.127589.

[32] H. Houben, H. Guillaud, Traité de construction en terre, Editions P, 1989.

[33] D. Silveira, H. Varum, A. Costa, T. Martins, H. Pereira, J. Almeida, Mechanical properties of adobe bricks in ancient constructions, Constr. Build. Mater. 28 (2012) 36–44, https://doi.org/10.1016/j.conbuildmat.2011.08.046.

[34] D. Muheise-Araalia, S. Pavia, Properties of unfired, illitic-clay bricks for sustainable construction, Constr. Build. Mater. 268 (2021), 121118, https://doi.org/10.1016/j.conbuildmat.2020.121118.

[35] Q.B. Bui, J.C. Morel, S. Hans, P. Walker, Effect of moisture content on the mechanical characteristics of rammed earth, Constr. Build. Mater. (2014), https://doi.org/10.1016/j.conbuildmat.2013.12.067.

[36] P. Walker, R. Keable, J. Martin, V. Maniatidis, Rammed Earth: Design and Construction Guidelines, IHS BRE, 2005.

[37] P.J. Walker, Strength, durability and shrinkage characteristics of cement stabilised soil blocks, Cem. Concr. Compos. 17 (1995) 301–310, https://doi.org/10.1016/0958-9465(95)00019-9.

[38] F. Rojat, E. Hamard, A. Fabbri, B. Carnus, F. McGregor, Towards an easy decision tool to assess soil suitability for earth building, Constr. Build. Mater. 257 (2020), 119544, https://doi.org/10.1016/j.conbuildmat.2020.119544.

[39] M.C. Jiménez Delgado, I.C. Guerrero, The selection of soils for unstabilised earth building: a normative review, Constr. Build. Mater. (2007), https://doi.org/10.1016/j.conbuildmat.2005.08.006.

[40] H. Van Damme, La Terre, un Béton d 'Argile, 2013, pp. 50–57.
[41] A. Perrot, D. Rangeard, F. Menasria, S. Guihéneuf, Strategies for optimizing the mechanical strengths of raw earth-based mortars, Constr. Build. Mater. (2018), https://doi.org/10.1016/j.conbuildmat.2018.02.055.
[42] C.M. Ouellet-Plamondon, G. Habert, Self-Compacted Clay based Concrete (SCCC): proof-of-concept, J. Clean. Prod. 117 (2016) 160–168, https://doi.org/10.1016/j.jclepro.2015.12.048.
[43] M. Moevus, Y. Jorand, C. Olagnon, S. Maximilien, R. Anger, L. Fontaine, L. Arnaud, Earthen construction: an increase of the mechanical strength by optimizing the dispersion of the binder phase, Mater. Struct. Constr. (2016), https://doi.org/10.1617/s11527-015-0595-5.
[44] A. Perrot, D. Rangeard, A. Levigneur, Linking rheological and geotechnical properties of kaolinite materials for earthen construction, Mater. Struct. Constr. (2016), https://doi.org/10.1617/s11527-016-0813-9.
[45] G. Landrou, C. Brumaud, F. Winnefeld, R.J. Flatt, G. Habert, Lime as an anti-plasticizer for self-compacting clay concrete, Materials (Basel) (2016), https://doi.org/10.3390/ma9050330.
[46] G. Landrou, C. Brumaud, M.L. Plötze, F. Winnefeld, G. Habert, A fresh look at dense clay paste: deflocculation and thixotropy mechanisms, Colloids Surf. A Physicochem. Eng. Asp. (2018), https://doi.org/10.1016/j.colsurfa.2017.12.029.
[47] G. Landrou, C. Brumaud, G. Habert, Influence of magnesium on deflocculated kaolinite suspension: mechanism and kinetic control, Colloids Surf. A Physicochem. Eng. Asp. (2018), https://doi.org/10.1016/j.colsurfa.2017.12.040.
[48] D. Ardant, C. Brumaud, G. Habert, Influence of additives on poured earth strength development, Mater. Struct. Constr. 53 (2020) 1–17, https://doi.org/10.1617/s11527-020-01564-y.
[49] Y. Du, G. Habert, C. Brumaud, Influence of tannin and iron ions on the water resistance of clay materials, Constr. Build. Mater. 323 (2022), 126571, https://doi.org/10.1016/J.CONBUILDMAT.2022.126571.
[50] T. Sedran, F. De Larrard, L. Le Guen, Détermination de la Compacité des Ciments et Additions Minérales à la Sonde de Vicat, n.d.
[51] F. de Larrard, T. Sedran, Optimization of ultra-high-performance concrete by the use of a packing model, Cem. Concr. Res. 24 (1994) 997–1009, https://doi.org/10.1016/0008-8846(94)90022-1.
[52] F. De Larrard, Concrete Mixture Proportioning, CRC Press, 1999, https://doi.org/10.1201/9781482272055.
[53] A. Lecomte, J.M. Mechling, Compacite des melanges et proprietes des grains, Bull. Des Lab. Des Ponts Chaussees (1999) 21–33.
[54] R.J. Flatt, P. Bowen, Yodel: a yield stress model for suspensions, J. Am. Ceram. Soc. 89 (2006) 1244–1256, https://doi.org/10.1111/J.1551-2916.2005.00888.X.
[55] N. Roussel, A. Lemaître, R.J. Flatt, P. Coussot, Steady state flow of cement suspensions: a micromechanical state of the art, Cem. Concr. Res. (2010), https://doi.org/10.1016/j.cemconres.2009.08.026.
[56] ISO - ISO 11277:2020 - Soil Quality — Determination of Particle Size Distribution in Mineral Soil Material — Method by Sieving and Sedimentation, (n.d.).
[57] ISO - ISO 17892-3:2015 - Geotechnical Investigation and Testing — Laboratory Testing of Soil — Part 3: Determination of Particle Density, (n.d.).
[58] Standard NF P94-068: Soils : Investigation and Testing — Measuring of the Methylene Blue Adsorption Capacity of a Rocky Soil — Determination of the Methylene Blue of a Soil by Means of the Stain Test, (n.d.).
[59] J.C. Santamarina, K.A. Klein, Y.H. Wang, E. Prencke, Specific surface: determination and relevance, Can. Geotech. J. 39 (2002) 233–241, https://doi.org/10.1139/t01-077.
[60] Y. Yukselen, A. Kaya, Comparison of methods for determining specific surface area of soils, J. Geotech. Geoenviron. Eng. 132 (2006) 931–936, https://doi.org/10.1061/(asce)1090-0241(2006)132:7(931).
[61] Y. Yukselen, A. Kaya, Suitability of the methylene blue test for surface area, cation exchange capacity and swell potential determination of clayey soils, Eng. Geol. 102 (2008) 38–45, https://doi.org/10.1016/j.enggeo.2008.07.002.
[62] A. Chiappone, S. Marello, C. Scavia, M. Setti, Clay mineral characterization through the methylene blue test: comparison with other experimental techniques and applications of the method, Can. Geotech. J. 41 (2004) 1168–1178, https://doi.org/10.1139/T04-060.
[63] E. Cokca, A. Birand, Determination of cation exchange capacity of clayey soils by the methylene blue test, Geotech. Test. J. 16 (1993) 518–524, https://doi.org/10.1520/GTJ10291J.
[64] A. Arrigoni, C.T.S. Beckett, D. Ciancio, R. Pelosato, G. Dotelli, A.C. Grillet, Rammed earth incorporating recycled concrete aggregate: a sustainable, resistant and breathable construction solution, Resour. Conserv. Recycl. 137 (2018) 11–20, https://doi.org/10.1016/j.resconrec.2018.05.025.
[65] G. Kahr, F.T. Madsen, Determination of the cation exchange capacity and the surface area of bentonite, illite and kaolinite by methylene blue adsorption, Appl. Clay Sci. (1995), https://doi.org/10.1016/0169-1317(94)00028-O.
[66] ISO - ISO 679:2009 - Cement — Test Methods — Determination of Strength, (n.d.).
[67] AENOR, UNE-EN ISO 17892-12:2019, Geotechnical Investigation and Testing - Laboratory Testing of Soil - Part 12: Determination of Liquid and Plastic Limits, UNE-EN ISO 17892-122019, 2019.
[68] J.C. Ruge, F. Molina-Gómez, E. Martínez-Rojas, L.A. Bulla-Cruz, J. Camacho-Tauta, Measuring the liquid limit of soils using different fall-cone apparatuses: a statistical analysis, Meas. J. Int. Meas. Confed. 152 (2020), 107352, https://doi.org/10.1016/j.measurement.2019.107352.
[69] ISO - ISO 17892-12:2018 - Geotechnical Investigation and Testing — Laboratory Testing of Soil — Part 12: Determination of Liquid and Plastic Limits, (n.d.).
[70] T.-W. Feng, A linear log d – log w model for the determination of consistency limits of soils, Can. Geotech. J. 38 (2001) 1335–1342, https://doi.org/10.1139/t01-061.
[71] D. Lootens, P. Jousset, L. Martinie, N. Roussel, R.J. Flatt, Yield stress during setting of cement pastes from penetration tests, Cem. Concr. Res. 39 (2009) 401–408, https://doi.org/10.1016/j.cemconres.2009.01.012.
[72] N.Q. Dzuy, D.V. Boger, Direct yield stress measurement with the vane method, J. Rheol. (N. Y. N. Y) (1985), https://doi.org/10.1122/1.549794.
[73] A.W. Saak, H.M. Jennings, S.P. Shah, The influence of wall slip on yield stress and viscoelastic measurements of cement paste, Cem. Concr. Res. (2001), https://doi.org/10.1016/S0008-8846(00)00440-3.
[74] A. Perrot, T. Lecompte, H. Khelifi, C. Brumaud, J. Hot, N. Roussel, Yield stress and bleeding of fresh cement pastes, Cem. Concr. Res. 42 (2012) 937–944, https://doi.org/10.1016/j.cemconres.2012.03.015.
[75] H. Van Olphen, An Introduction to Clay Colloid Chemistry, for Clay Technologists, Geologists, and Soil Scientists, 1977, https://doi.org/10.1002/jps.2600530238.
[76] E. Tombácz, M. Szekeres, Colloidal behavior of aqueous montmorillonite suspensions: the specific role of pH in the presence of indifferent electrolytes, Appl. Clay Sci. (2004), https://doi.org/10.1016/j.clay.2004.01.001.
[77] D. Ardant, C. Brumaud, G. Habert, Tackling variability of clay to provide a robust binder, in: Bio-based Build. Mater., 2022, pp. 382–387, https://doi.org/10.4028/www.scientific.net/cta.1.382.
[78] A. Mesbah, J.C. Morel, M. Olivier, Clayey soil behaviour under static compaction test, Mater. Struct. Constr. 32 (1999) 687–694, https://doi.org/10.1007/bf02481707.
[79] H. Van Damme, M. Zabat, J.-P.-.P. Laurent, P. Dudoignon, A. Pantet, D. GÃlard, H. Houben, N. Agnew, Nature and distribution of cohesion forces in earthen building materials, in: Proc. Second Int. Conf. Conserv, Grotto Sites, 2004.
[80] T. Fitton, K. Seddon, Relating Atterberg limits to rheology, in: Proc. 15th Int. Semin. Paste Thick. Tailings, Australian Centre for Geomechanics, Perth, 2012, pp. 273–284, https://doi.org/10.36487/acg_rep/1263_23_fitton.
[81] F. Mahaut, X. Chateau, P. Coussot, G. Ovarlez, G.O. Yield, Yield stress and elastic modulus of suspensions of noncolloidal particles in yield stress fluids, J. Rheol. (N. Y. N. Y) 52 (2008), https://doi.org/10.1122/1.2798234ï.
[82] Z. Toutou, N. Roussel, Multi Scale Experimental Study of Concrete Rheology: From Water Scale to Gravel Scale, Mater. Struct. 39 (2006) 189–199, https://doi.org/10.1617/S11527-005-9047-Y (2006 392).
[83] J. Yammine, M. Chaouche, M. Guerinet, M. Moranville, N. Roussel, From ordinary rhelogy concrete to self compacting concrete: a transition between frictional and hydrodynamic interactions, Cem. Concr. Res. 38 (2008) 890–896, https://doi.org/10.1016/J.CEMCONRES.2008.03.011.
[84] F. Mahaut, S. Mokéddem, X. Chateau, N. Roussel, G. Ovarlez, Effect of coarse particle volume fraction on the yield stress and thixotropy of cementious materials, Cem. Concr. Res. 38 (2008) 1276–1285, https://doi.org/10.1016/J.CEMCONRES.2008.06.001.